PERGAMON

International Journal of Heat and Mass Transfer 42 (1999) 1–12

International Journal of HEAT and MASS TRANSFER

Comparison of steady state and transient methods for measurement of local heat transfer in plate fin-tube heat exchangers using liquid crystal thermography with radiant heating

R. E. Critoph*, M. K. Holland, M. Fisher

Engineering Department, University of Warwick, Coventry CV4 7AL, U.K.

Received 23 June 1997; in final form 6 July 1998

Abstract

Optical methods for measuring local heat transfer coefficients using thermochromic liquid crystals are discussed. Two techniques using radiative steady state and transient heating have been used to measure local heat transfer on the fin of a plate fin-tube heat exchanger. It is estimated that the errors in the steady state technique should be no more than $\pm 10\%$ and the results are given. The mean value of the heat transfer coefficient over the whole surface is 35 W m^{-2} K^{-1}, rising to 73 W m^{-2} K^{-1} at the leading edge. The transient method does not give results consistent with the steady state method when heat transfer coefficients are based on the fluid inlet temperature. It is suggested that the steady state method is preferable since it yields numerical values that are closer to those based on local temperature and hence easier to interpret when observing the effects of changing the local surface geometry.

Nomenclature

c_p specific heat of glass [J kg^{-1}K^{-1}]
h heat transfer coefficient based on inlet temperature [W m^{-2} K^{-1}]
h_{local} heat transfer coefficient based on local bulk temperature [W m^{-2} K^{-1}]
H nominal heat transfer coefficient defined by equation (5) [W m^{-2} K^{-1}]
k thermal conductivity of glass sheet [W m^{-2}K^{-1}]
q heat flux [W m^{-2}]
q_{ab} radiation heat flux absorbed by upper liquid crystal layer [W m^{-2}]
q_{cond_z} heat flux conducted through middle glass sheet [W m^{-2}]
$q_{cond_{xy}}$ heat flux conducted along middle glass sheet [W m^{-2}]
s distance along a streamline from the leading edge [m]
t time taken to reach transition temperature [s]
T temperature [K]
x, y directions in the plane of the glass sheet [m]
z thickness of glass sheet [m].

Greek symbols

ε emissivity
ρ density of glass sheet [kg m^{-3}]
σ Stephen–Boltzmann constant, 56.7×10^{-9} W m^{-2} K^{-4}.

Subscripts

a air inlet
bot lower liquid crystal surface
conv convective
k liquid crystal surface
g glass
rad net radiative
tot total
wall wall.

* Corresponding author. Tel.: 0044 1203 523 523; fax: 0044 1203 418922

0017–9310/98/$—see front matter
PII: S0017–9310(98)00207–5

1. Introduction

Many methods that have been used to determine local heat transfer coefficients on surfaces, including the use of thermally sensitive paints, volatile solids, etc. Our particular interest in the performance of plate fins found in plate fin-tube heat exchangers used as air conditioning condensers or evaporators. A typical condenser uses 10 mm o/d(3/8 inch) tubes in a 25.4 mm (1 inch) equilateral triangular pitch. The fins are normally pressed from 0.12 mm aluminium coil and the air passageways between them can be as little as 1.2 mm wide. We require a means of easily observing the local heat transfer and of comparing the mechanisms and effect of surface modifications such as vortex generators.

The two main methods that have been used to determine local heat transfer are:

- Constant heat flux surfaces with thermocouple arrays in a steady state condition, as reported by Eibeck and Eaton [1], Yanagihara and Torii [2] and Pauley and Eaton [3].
- The use of thermochromic liquid crystals in transient heating, as reported by Jones [4], Tiggelbeck et al. [5, 6] etc.Their method subjects a test surface to a step change in fluid flow temperature. The length of time taken for the liquid crystals at a certain location to reach a particular temperature(denoted by a colour change) is related to the heat transfer at that location.

The use of an optical technique offers advantages of flexibility, it being comparatively easy to alter the geometry of the surface being studied and so liquid crystal thermography was chosen as best suited to our needs. The following three ways in which liquid crystals may be used to obtain heat transfer coefficients were selected for comparison.

(1) Transient heat transfer with a thick wall.
(2) Transient heat transfer with a thin wall.
(3) Steady state heat transfer.

The first two methods are compared by Valencia et al. [7]. Both methods subject the surface being studied to a step change in fluid flow temperature and analyse the transient response, but in the first method the surface is considered to be the boundary between the flow and a wall of semi-infinite thickness, whilst in the second method the wall is assumed thin enough that it may be considered isothermal in the direction normal to its surface. The latter method is show to have certain advantages.

Steady state heat transfer with a constant flux density is conceptually simple and easy to analyse but the provision of a constant flux surface poses experimental difficulties. The use of electrically heated foils is possible, but uniform flux density can be difficult to achieve in practice. This work examines the practicability of using a radiative source to heat the surface.This has the advantage that it is easy to change the surface geometry so that many different tests may be carried out in a comparatively short time. After using the steady state radiative heating approach described in detail below, a transient radiative heating method was used which, it was hoped, would reduce the test time.

2. Steady state measurement technique and theory

The method developed employs a powerful uniform light source to heat the surface directly by absorption. The liquid crystals are on a black substrate (absorptivity estimated to be 0.95) and the absorbed flux density is calculated from the measured transmissivity of the top glass sheet and incident radiation. The configuration chosen for evaluation is shown in Fig. 1.

Two air flow channels are used rather than one, since in the steady state the total radiative heat flux is known to be dissipated in the two air streams rather than to the surrounding ambient air. (If one flow channel were used it would be difficult to correlate the heat flux and air flow at any single point due to heat losses). If the fin geometry is flat then the heat transfer coefficient can be assumed equal on the top and bottom surface of the centre fin at a particular location. The heat transfer coefficient can be calculated there, given the heat flux, the fin thermal resistance, the local fin temperature and reference temperature such as that of the inlet air. The liquid crystals on the top surface of the centre fin indicate when the local fin temperature is in the transition range. A test at a particular flux density gives rise to a particular colour contour on the surface, which corresponds to a particular heat transfer coefficient. A series of such tests at different flux densities reveal the heat transfer coefficient at a range of locations.

In the case of an asymmetric geometry, such as a wavy fin, with differing top and bottom heat transfer coefficients, both the top and bottom surfaces of the central fin need to be covered with the liquid crystals. Temperatures can be measured on both surfaces for a range of heating flux densities, and the separate top and bottom coefficients can be derived as a function of the normal top and bottom coefficients. The experiments reported here have all been carried out with flat fins. In these experiments the thermal resistance in the fin in the z-direction is only a few percent of the convective resistance.This would make it very difficult to differentiate between the top and bottom heat transfer coefficients of a wavy fin with any accuracy.

With reference to Fig. 1., the energy flows are all calculable. The radiant energy absorbed by the upper liquid crystal layer is q_{ab} W m^{-2}. An energy balance for the upper surface is:

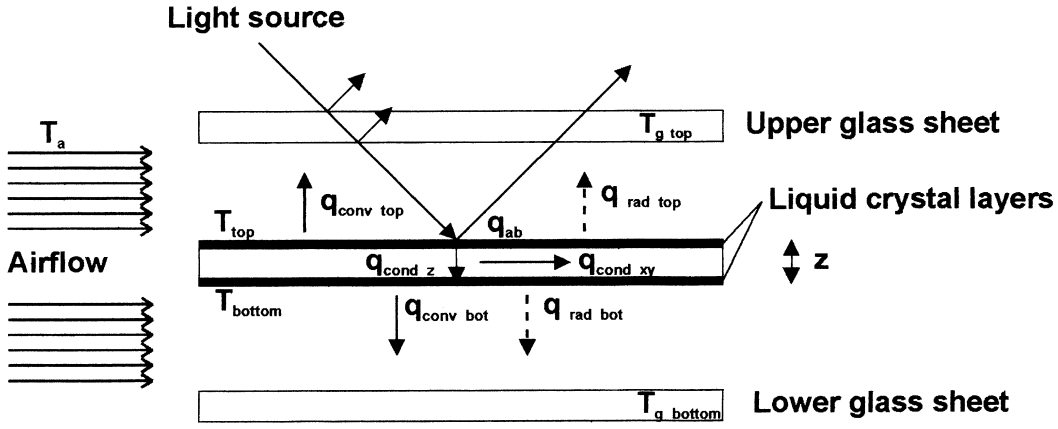

Fig. 1. Energy flows in test section.

$$q_{ab} = q_{conv\,top} + q_{rad\,top} + q_{cond\,z} + q_{cond\,xy}$$
$$= q_{conv\,top} + q_{rad\,top} + \frac{k(T_{top} - T_{bot})}{z} + kz\left(\frac{\partial^2 T}{\partial x^2} + \frac{\partial^2 T}{\partial y^2}\right) \quad (1)$$

The energy balance for the lower surface is:

$$q_{cond\,z} = q_{conv\,bot} + q_{rad\,bot} \quad (2)$$

The top and bottom surface convective heat fluxes are given by a heat transfer coefficient based on the difference between the air inlet and surface temperatures:

$$q_{conv} \equiv h(T - T_a) \quad (3)$$

The net low temperature radiation exchange between the middle and top or middle and bottom sheets respectively is given by:

$$q_{rad} = \frac{\sigma(T^4 - T_g^4)}{1/\varepsilon_{lc} + 1/\varepsilon_g - 1} \quad (4)$$

In order to calculate h_{top} or h_{bot} at a location the radiation fluxes and conductive flux in the plane of the sheet need to be known. They are both typically an order of magnitude or more below the convective fluxes and so they do not need to be known with great precision.

The conduction term was estimated using a computer model of the system which took as its input parameters the local heat transfer coefficients corrected for radiation loss but not for conduction, the radiation boundary conditions, the glass thickness and conductivity. Using a simple two-dimensional model of conduction in the glass an estimate of the error was derived. Typical values are reported with the results below.

Evaluation of the radiation terms require a knowledge of the emissivities of both the glass and liquid crystal surfaces and of their temperatures. The appropriate liquid crystal temperature is that of the chosen colour band. The red band chosen had a temperature of 35.1°C. Any drift in the properties of the crystals was monitored by two 5 μm thick K-type foil thermocouples on the upper and lower surfaces, bonded between the liquid crystal layer and glass. The thermocouples had in turn been calibrated to within 0.1°C against a standard mercury-in-glass thermometer. The temperature of the lower surface liquid crystal will not be equal to that of the upper, but is typically only 0.3°C cooler, resulting in little error of the radiation flux. The emissivity of the glass was taken as 0.93[10]. That of the liquid crystal was measured approximately using an infra-red thermometer with an emissivity calibration adjustment. The measurements implied an emissivity of 0.97 when apparently black and 0.95 when apparently red. The latter value was used. The temperature of the top glass sheet was estimated as being a weighted average of 2/3 the liquid crystal temperature and 1/3 the ambient temperature. This estimate was checked with a single fine wire thermocouple stretched across the top glass surface with its junction in contact with the glass. With an incident radiation of 550 W m^{-2} the measured glass temperature was 28.4°C compared with an estimated value of 31.3°C. The error in the estimated radiation exchange between the top and central sheets was 3% of the incident radiation. Later experiments will measure the temperature with a non-contact thermometer. The radiation heat transfer between the surfaces is typically 30 W m^{-2}.

These 'loss' terms are deducted from q_{ab} to give the convection flux from both top and bottom surfaces $q_{conv\,tot}$. The calculation of the coefficients varies depending upon whether the fin is symmetrical with the same coefficient expected on both top and bottom surfaces. It also depends upon whether the thermal resistance through the middle sheet is significant. Suppose the resistance to be significant and the top and bottom surfaces to have a different h. Two sets of contours are obtained, one from the top layer of liquid crystals and one from the

bottom layer. Two nominal heat transfer coefficients based on the air inlet temperature are calculated,being defined by:

$$H = \frac{q_{\text{conv tot}}}{T_a - T_{lc}}$$

$$H' = \frac{q'_{\text{conv tot}}}{T'_a - T'_{lc}} \tag{5}$$

The use of a prime (′) indicates the use of contours on the bottom surface. In obtaining both sets of contours radiant heating is applied to the top surface only.

Analysis of the thermal resistance networks applying to both cases at the same location gives the heat transfer coefficients at the top and bottom surfaces, based on inlet temperature, as a function of the properties of the middle glass sheet, H andH':

$$h_{\text{top}} = H + \frac{k}{z}\left(\frac{H}{H'} - 1\right), \quad h_{\text{bot}} = \frac{k}{z}\left(\frac{H'}{H} - 1\right) \tag{6}$$

In the experiments reported here both flow channels are identical also h_{top} and h_{bot} are equal. This enables the solution of h either as a function of H and H', in which case the thermal resistance of the glass is not needed or as a function of H and k/z in which case only the top set of contours need to be measured:

$$\frac{1}{h} = \frac{1}{H} + \frac{1}{H'} \tag{7}$$

$$h = \frac{H}{2} - \frac{k}{z} + \sqrt{\left(\frac{k}{z}\right)^2 + \left(\frac{H}{2}\right)^2} \tag{8}$$

The latter method was chosen both for convenience and because the results are not a strong function of k/z. Equation (8) may be expressed implicity as:

$$h = \frac{H}{1 + \left(\dfrac{1}{1 + \dfrac{hz}{k}}\right)} \tag{9}$$

In the case of the 0.7 mm glass used an error of 10% in k/z with a typical h of 40 W m^{-2} K^{-1} only changes h by 0.2%. If the thermal resistance of the central plate is small then h tends to $H/2$. In our experiments, where the top and bottom heat transfer coefficients are equal, and if transverse conduction effects are neglected:

$$H = \frac{q_{ab} - q_{\text{rad top}} - q_{\text{rad bot}}}{T_a - T_{lc}} \tag{10}$$

3. Experimental equipment

The experimental equipment used is illustrated in Fig. 2. The fin under investigation is enclosed between two similar fins, providing two airflow channels 2 mm in

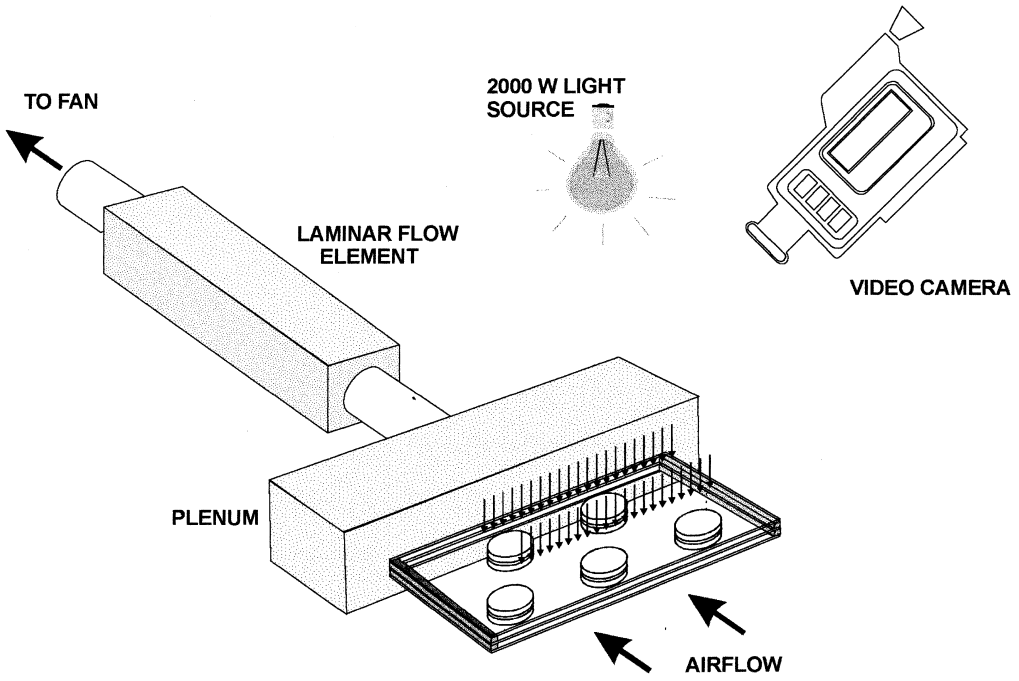

Fig. 2. Experimental apparatus.

height and 44 mm deep.This is the full size of the air channels in a particular commercial two row air conditioning condenser. The three fins are constructed from 0.7 mm thick glass sheets. The centre fin has a layer of liquid crystals applied to both surfaces. The crystals used had a full visible spectrum range of 1°C and the red band used had a range of about 0.1°C. The three layers are held together with spacers ensuring the correct fin spacing is maintained. Extensions of these spacers are used to support the three fin assembly in front of the aperture in the aluminium manifold. The outer surfaces are held very close to the manifold and the gap is sealed with adhesive tape. The aluminium manifold chamber is connected via a length of pipe to the laminar flow element, which in turn is connected to a fan plenum chamber. A laminar flow element is employed to measure the cooling air flow rate and provides a linear pressure drop signal increasing with volumetric flow. Air is drawn through the assembly by the fan connected to the plenum chamber. The air speed in the core was maintained at 2 m s^{-1} in all tests, this being the speed used in the commercial heat exchanger being modelled. The corresponding Reynolds number based on the channel height is 265.

The uppermost liquid crystal layer on the central glass sheet is heated by absorbing the light which passes through the upper glass sheet. The light used is a 2000 W tungsten photographic flood lamp selected for its high output and even distribution. The light is equipped with an electronic unit to control its brightness and a ground glass diffuser that absorbs the great majority of the infra red. The light source is calibrated with a Kipp and Zonen CM5 solarimeter, using a covering sheet of glass fin material to correct for the transmission losses due to the top glass fin. The area of interest exhibited a variation of radiation flux across it of less than $\pm 1\%$. This compares favourably with electric surface heaters investigated by Jambunathan et al. [8]. They reported a $\pm 4.5\%$ variation for carbon sheet heaters, $\pm 12\%$ for gold foil and $\pm 30\%$ for stainless steel. The incident heat flux has to be multiplied by the liquid crystal absorptivity to yield the heat flux at the surface.Reflected light is assumed to leave the system without further absorption by the top glass sheet. The absorptivity is estimated as 0.95 which means that the likely levels of absorption in the top sheet will not lead to significant errors.

A Cannon EX2 Hi8 camcorder equipped with a CL8-120 mm zoom lens is used to photograph the crystals as they change colour due to temperature change.

The liquid crystals used are supplied by Hallcrest in the form of self adhesive 125 micron polyester sheets, with a pressure sensitive adhesive backing. this is easily applied to the flat fin surfaces, but the more typical spray application would be required for alternative geometries. The crystal range selected (R35C1W) undergoes a full colour transition over the range of 35–36°C. The initial black to red transition at 35.1°C was selected to mark the isotherms since it is the most easily recognised by eye.

The pictures of the liquid crystals are converted from the Hi8 camcorder tape to a high definition 736×560 pixel 256 colour GIF by using a frame grabber card installed in a P.C. In order to select the required isotherm, and correct the image due to the offset camera position the following method has been devised.

(1) The GIF is imported into a graphical manipulation package, such as Corel draw.
(2) Ellipses are drawn around the ends of the tubes, the sizes and positions of these ellipses are measured and recorded.
(3) The geometric translations required to correct the equilateral triangular pitch of these tube ends is calculated.
(4) The isothermal line is traced by eye and a line is drawn over the image using the graphics package.
(5) The calculated geometric translations are applied to the whole image.
(6) The applied translations are checked by ensuring that the ellipses are now circular and the tube pitch geometry is correct.
(7) A rectangle representing the region of interest is drawn onto the image.
(8) The original GIF image and drawn ellipses/circles are deleted.
(9) The remaining isotherm and rectangle are saved to disc as a GIF.

In order to calculate the heat transfer coefficients at all points on the surface of the fin, a Matlab program has been written which imports the GIF files previously saved to disk.Each GIF file has one isotherm stored in it.

Using Matlab a matrix is set up to represent the region of interest of the fin surface to a specified resolution. The imported GIF isotherms and their associated nominal heat transfer coefficients, are then combined using the GRIDDATA function in Matlab. This function uses an inverse distance method to interpolate between the differently spaced isotherms, producing a value of the nominal heat transfer coefficient for each point on the regularly spaced grid at the specified resolution.

4. Steady state results

The results presented here are obtained using the steady state method described above. The actual GIF (256 colour reduced to black and white for reproduction in this paper) produced from the frame grabber card is shown in Fig. 3. The actual resolution of this image is 736×560 pixels. The corresponding reduced colour GIF containing the isotherm and the test section outline with ellipses is shown in Fig. 4. The original GIF image is then deleted leaving the distorted outline, ellipses and isotherm as shown in Fig. 5. After applying the correct geometric

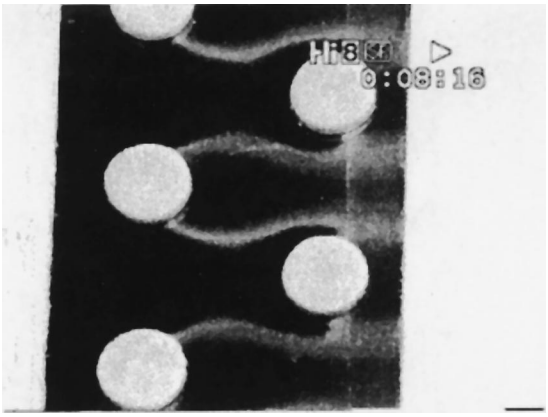

Fig. 3. Original colour GIF.

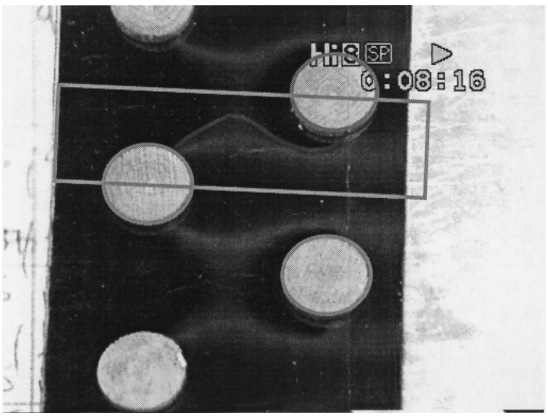

Fig. 4. GIF with ellipses, region of interest and isotherm added.

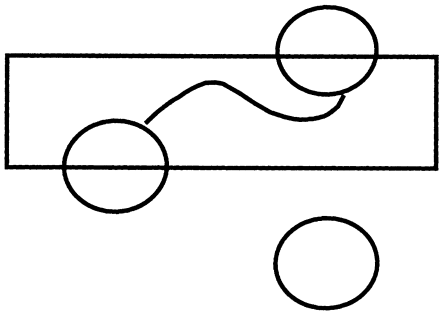

Fig. 5. Distorted isotherm and region of interest.

transformations the rectangular region of interest evolves with the true shape of the isotherm and the ellipses are transformed to circles as shown in Fig. 6. Deleting the circles leaves only the region of interest and isotherm to be imported into Matlab with the corresponding nominal heat transfer coefficient (Fig. 7).

Figure 8 shows some of the original GIFs for different flux densities. Figure 9 shows a 3D plot of the heat transfer coefficients over the surface of the fin. The very high coefficient at the leading edge demonstrates the effect of the very thin developing boundary layer in this region. The mean value of the heat transfer coefficient over the whole surface is 35.1 W m^{-2} K^{-1}. This may be compared with the experimental result of 45.4 W m^{-2} K^{-1} [8] on a condenser core with the same geometry. The boundary conditions are of course different, since the experimental results were for condensing (isothermal) refrigerant within the tubes, and the present results are for a uniform radiative heat flux on the fins.

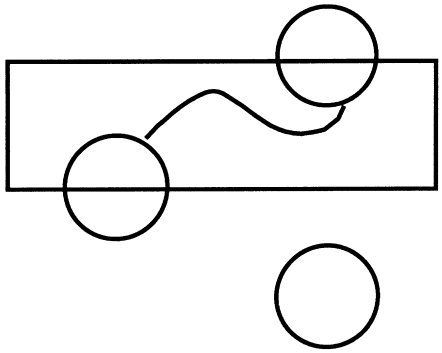

Fig. 6. Corrected isotherm and outline.

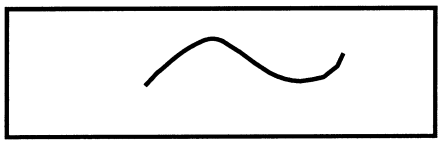

Fig. 7. GIF ready for import into Matlab.

4.1. Estimate of accuracy

As will all liquid crystal thermography methods it is quite difficult to determine the actual position of the relevant isotherm/colour fringe. Using a controllable intensity light source to heat the surface results in the apparent colours of the crystals changing during the experiment even though the temperature may remain constant. This effect can be minimised by using the edge of the black to red transition as the isotherm, but even then it makes automatic selection of the isotherm using computational techniques difficult. Thus a manual technique has been applied in order to select the isotherms. The uncertainty of the actual fringe position and the geometric compensation required for the camera viewing angle gives rise to a possible positional error for the fringe in the order of 0.5 mm. The light intensity itself is not perfectly uniform and varies by $\pm 1\%$ over the fin area considered. The main source of inaccuracy however is the determination of the temperature to be used to calculate the temperature difference on which the nominal

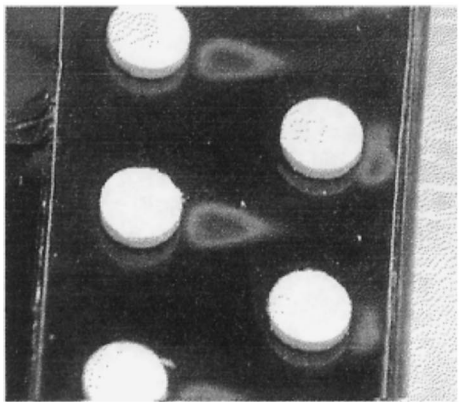

q = 581.9 W/m²

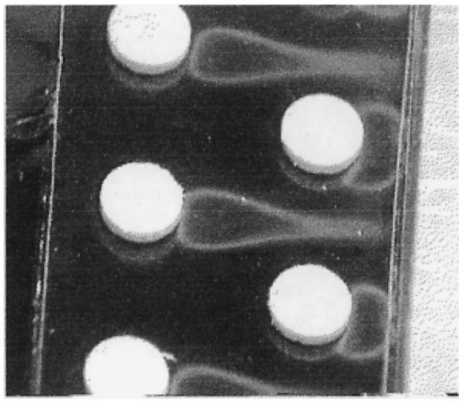

q = 625 W/m²

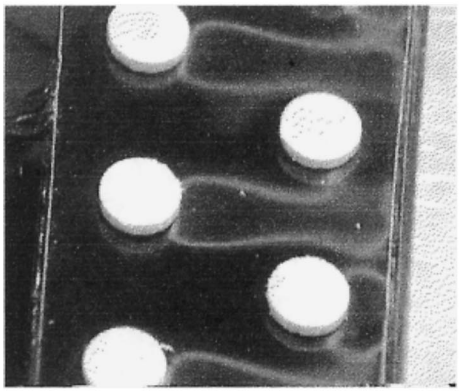

q = 653.4 W/m²

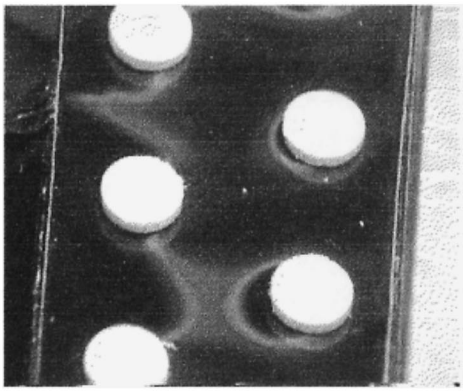

q = 819 W/m²

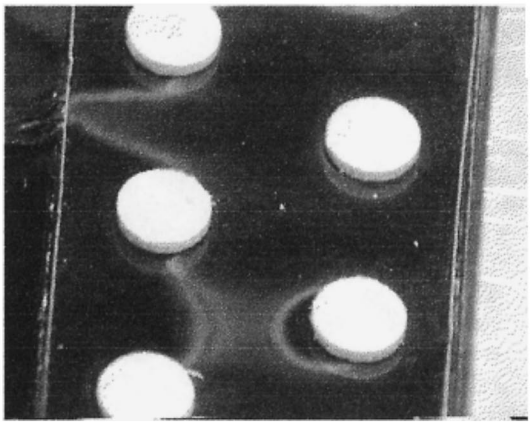

q = 1034.5 W/m²

Fig. 8. Contours obtained in steady state tests.

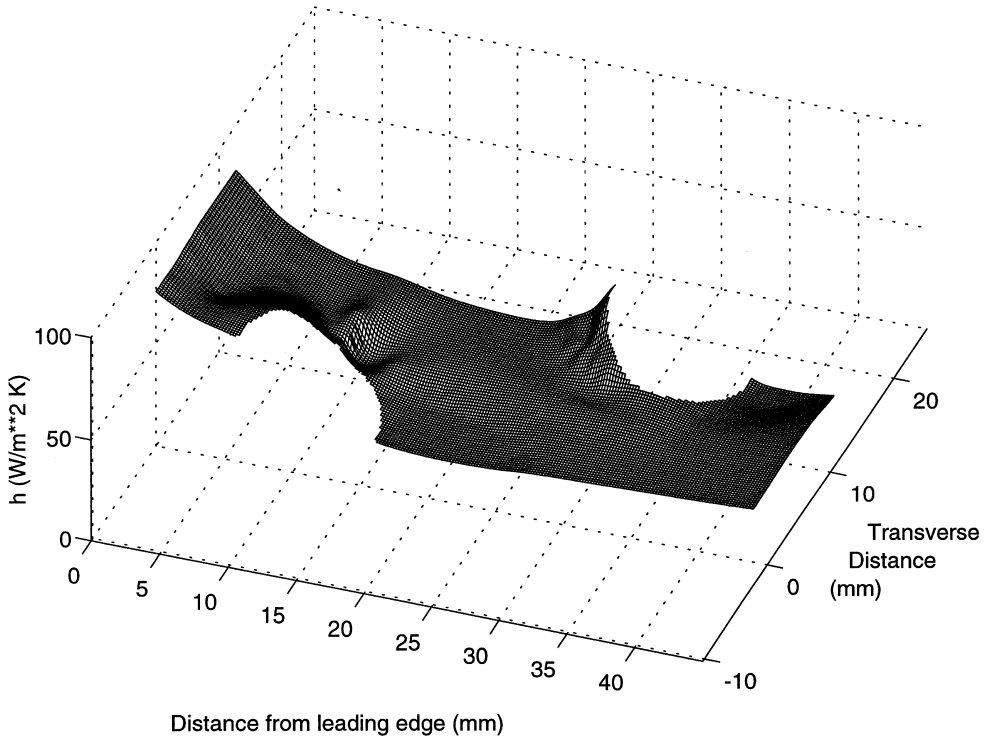

Fig. 9. Local heat transfer coefficients measured using steady state technique.

heat transfer coefficient is to be based. With temperature differences of approximately 8–10°C errors in the order of ±0.5°C result in errors of ±5–6% in the determination of the heat transfer coefficient. Errors in the estimation of radiation losses (discussed above) may add a further 1% uncertainty. The tangential conduction was calculated using a two-dimensional conduction model of the glass sheet and assuming the measured local coefficients to be correct. The proportional difference made to the local heat transfer coefficients depends upon the local value of the second derivative of the glass temperature with respect to distance. This is greatest near the leading edge. The overall effect of tangential conduction is to smooth out any local variations in heat transfer coefficient and so its effect is also a function of the resolution used. Table 1 illustrates the effect of tangential conduction on the calculated local heat transfer coefficient for three locations and two resolutions. For locations more than one or two mm from the leading edge and a resolution of 0.4 mm the error is less than 2%.

5. Transient measurement technique

The steady state technique requires the recording of up to ten contours, each of which may need 20 min to establish. An alternative approach is to try to use the information contained within the results of a single transient test using the same apparatus. The fan is switched on and adjusted until the desired flow velocity is obtained. Then the light source is suddenly applied at a high flux density. A continuous video recording of the moving colour contours is made as they progress from the 'hot spots' in areas of poor heat transfer outwards until they sweep up to the leading edge where the heat transfer is highest. In principle the time taken for the colour change to reach any location is related to the local heat transfer coefficient.

The middle glass sheet is a 'thin' wall in that its Biot number is 0.02 when the local heat transfer coefficient is 100 W m^{-2} K^{-1}. This allows it to be treated as an isothermal lumped system in the z direction. Radiation was treated in the same way as for the steady state tests. No correction was made for transient tangential conduction.

The solution to the transient heat flow equation with the lumped system approximation with equal top and bottom heat transfer coefficients based on inlet air temperature is:

$$h = \frac{-\rho c_p z}{2t} \ln\left(1 - \frac{2h}{q_{\text{conv tot}}}(T_{lc} - T_a)\right) \tag{11}$$

This equation may be solved iteratively.

Table 1
Variation in conduction correction factor with position and resolution

Distance from leading edge (mm)	Percentage correction factor for 0.2 mm × 0.2 mm resolution	Percentage correction factor for 0.4 mm × 0.4 mm resolution	Corrected heat transfer coefficient [W m^{-2} K^{-1}]
1	18.3	4.0	73.3
2.5	2.9	—	59.8
15.4	5.5	1.4	37.0
24.3	1.0	0.4	37.0

6. Transient test results and comparison with steady state results

A set of transient contours were recorded using the same experimental apparatus and are shown in Fig. 10. They appear significantly different in shape to those of the steady state tests. Figure 11 shows the plot of local heat transfer coefficients calculated using equation (11). They are very different to those of the steady state tests and in particular show a rising heat transfer coefficient towards the trailing edge, which is physically most unlikely. Upon investigation it appeared that the differences between the two were greater towards the trailing edge (up to 50%) and that they were due to differing local bulk air temperatures in the two tests. The actual convective heat flux at a location is a function of the flow temperature gradient normal to the wall at that location. In the steady and transient tests, which had the same flow fields, the local air temperatures are very different when the wall temperatures reach the colour transition level.

When defining the heat transfer coefficient using the steady state technique the air inlet temperature is used. The total power input from the fin to the air up to some location s along a streamline is:

$$q_{\mathrm{conv}}(s) = \int_0^s h[T_{\mathrm{wall}} - T_{\mathrm{a}}(0)]\,\mathrm{d}s \tag{12}$$

The power input to s can also be given by a heat transfer coefficient h_{local} based on the locally varying value of the bulk air temperature:

$$q_{\mathrm{conv}}(s) = \int_0^s h_{\mathrm{local}}[T_{\mathrm{wall}} - T_{\mathrm{a}}(s)]\,\mathrm{d}s \tag{13}$$

When the same radiant flux and location are being considered, the integrals must have the same values but the numerical values of h_{local} will all be higher than h since the temperature difference is less. It is usual to use the coefficient based on inlet temperature since the bulk temperature is in general not known. Using the steady state technique in this experiment does not give large differences in the numerical value of h and h_{local} because the rise in temperature of the air passing through the heat exchanger is not large. When obtaining contours for regions of low heat transfer at the trailing edge, low heat fluxes are used and the rise in temperature might be 5°C (averaged over the test section) when there is a 15°C difference between the wall and inlet temperatures. The hypothesis is that in the transient tests the local bulk temperature at the trailing edge at transition is less than that in the steady state, giving a higher heat transfer coefficient based on inlet temperature. This hypothesis could be tested by analysis of a stream tube flowing from the leading to the trailing edge. Knowing h and $q_{\mathrm{conv\,tot}}$ an energy balance on the air in the tube between the leading edge and some distance s along it would enable the bulk air temperature to be calculated at s. The heat transfer coefficient based on the local bulk air temperature h_{local} could then be calculated. This should be consistent with a similar analysis carried out on the transient data to determine h_{local}. Unfortunately, the flow pattern in the plate fin-tube test piece is not known and so the analysis cannot be carried out. As an alternative test, the 'tubes' were removed so that simple dimensional channel flow resulted. Steady state and transient tests were repeated and the values of h_{local} compared.

7. Technique comparison with 2D channel flow

The local heat transfer coefficient based on inlet temperature using steady state measurement is shown in Fig. 12, together with a theoretical curve taken from Kays and Crawford [9]. A simple finite difference computer program was used to determine the local bulk temperature, which was in turn used to calculate the local heat transfer coefficient based on that temperature. They diverge as the heated length increases. The local coefficient obtained from the steady state test is then used to predict the local coefficients based on inlet temperature and times to transition in a transient test. The simulated time and actual times are shown in Fig. 13. The agreement is good near to the leading edge but diverges towards the trailing edge as integrated errors accumulate.

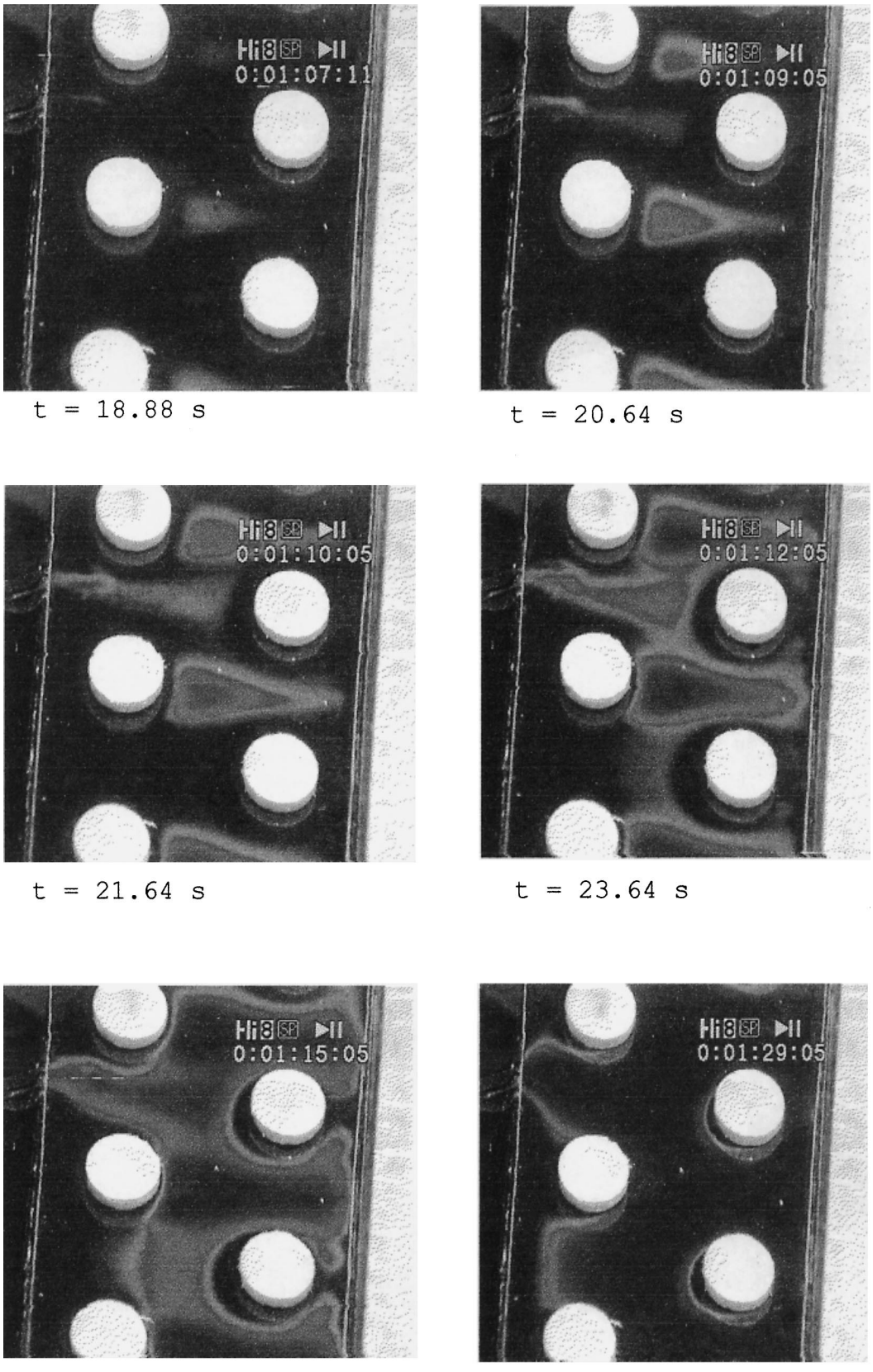

Fig. 10. Contours obtained in transient tests.

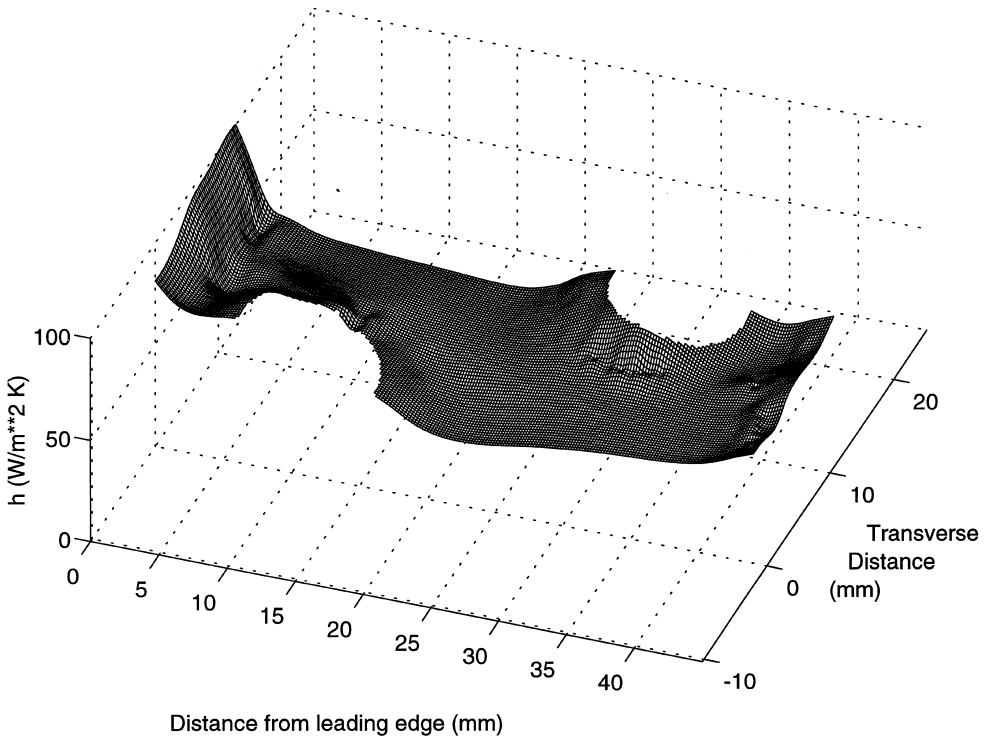

Fig. 11. Local heat transfer coefficients measured using transient technique.

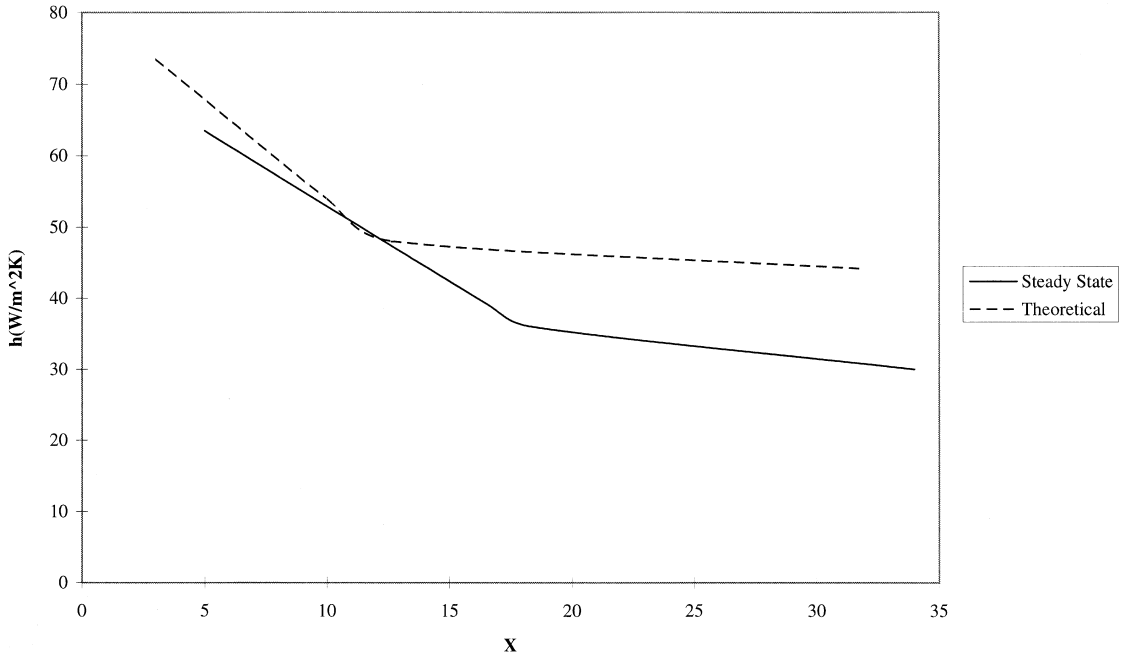

Fig. 12. Local heat transfer coefficients in 2D channel flow.

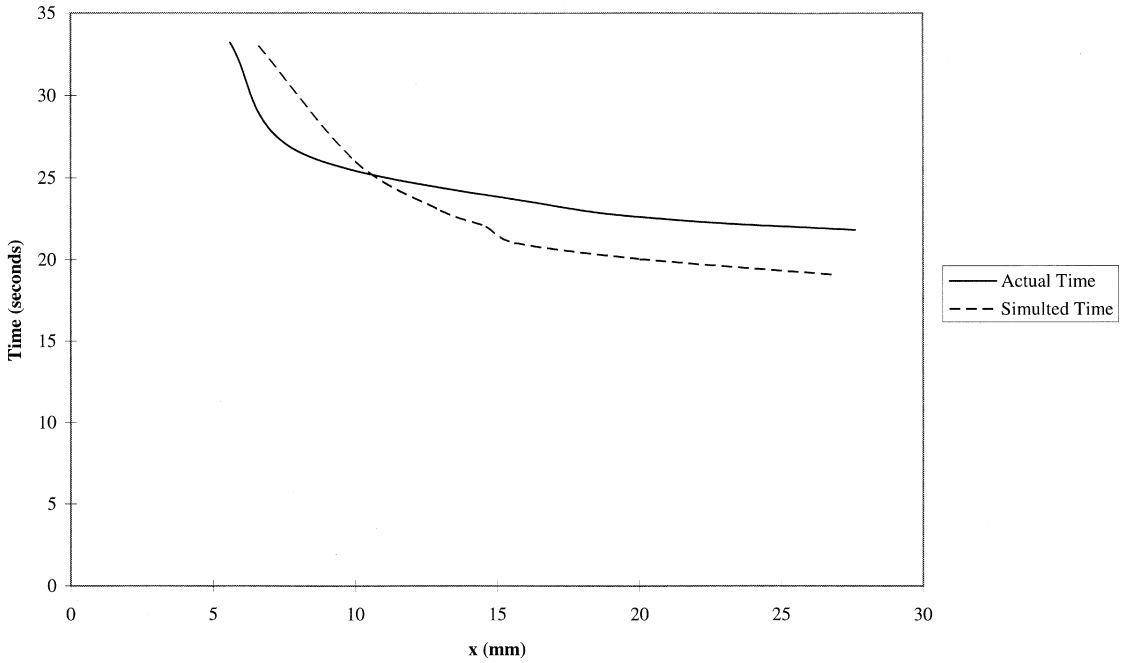

Fig. 13. Predicted and actual transition times in channel flow transient test.

8. Conclusions

A novel method of using radiant heating with liquid crustal thermography to measure local heat transfer coefficients has been described. Either steady state or transient tests may be used to derive coefficients but they are not comparable when based on inlet air temperatures. Whilst basing the heat transfer coefficients on local temperatures does not totally reconcile the results of transient and steady state tests it is seen to provide a satisfactory explanation for most of the discrepancy. The steady state method is preferred since it yields numerical values that are closer to those based on local temperature and hence easier to interpret when observing the effects of changing the local surface geometry.

Acknowledgements

This paper is based on work funded by EPSRC Grant GR/J45954 and Lennox Industries Ltd.

References

[1] P.A. Eibeck, J.K. Eaton, Heat transfer effects of a longitudinal vortex embedded in a turbulent boundary layer, ASME J. of Heat Transfer 109 (1987) 16–23.

[2] J.I. Yanagihara, K. Torii, Enhancement of laminar boundary layer heat transfer by a vortex generator, JSME Int. J., Series II 35 (1992) 400–405.

[3] W.R. Pauley, J.K. Eaton, The effect of longitudinal embedded vortex arrays on turbulent boundary layer heat transfer, ASME J. of Heat Transfer 116 (1996) 871–879.

[4] T.V. Jones, S.A. Hippensteele, High resolution heat transfer coefficients maps applicable to compound surfaces using liquid crystals in transient wind tunnels, Proceedings of the 24th ASME/AIChE National Heat Transfer Conf., ASME HTD 71 (1987) 1–9.

[5] St. Tiggelbeck, N.K. Mitra, M. Fiebig, Experimental investigations of heat transfer enhancement and flow losses in a channel with double rows of longitudinal vortex generators, Int. J. Heat mass Transfer 36 (9) (1993) 2327–2337.

[6] St. Tiggelbeck, N.K. Mitra, M. Fiebig, Comparison of wing type vortex generators for heat transfer in channel flows, ASME J. Heat Transfer 116 (1996) 880–885.

[7] Valencia, M. Fiebig, N.K. Mitra, Influence of heat conduction on determination of heat transfer coefficient by liquid crystal thermography, Experimental Heat Transfer 8 (4) (1995) 271–279.

[8] R.E. Critoph, M.K. Holland, L. Turner, Heat Transfer Measurements of air-cooled plate fin-tube air conditioning condensers using a refrigerant thermosyphon, Int. J. Refrigeration 19 (6) (1996) 400–406.

[9] W.M. Kays, K.E. Crawford, Convective Heat and Mass Transfer, McGraw-Hill, 1980.

[10] F. Kreith, W.Z. Black, Basic Heat Transfer, Harper and Row, 1980.